Int J Adv Manuf Technol (2006) 28: 966–977
DOI 10.1007/s00170-004-2444-5

ORIGINAL ARTICLE

G. Celano · A. Costa · S. Fichera

Statistical design of variable sample size and sampling interval $\bar{X}$ control charts with run rules

Received: 11 February 2004 / Accepted: 13 October 2004 / Published online: 13 July 2005

Abstract In this paper, improved Shewhart control charts based on hybrid adaptive and run rule schemes are introduced to enhance the statistical performances of the traditional static scheme, designed with consideration given to the fixed values of sample size, the width of the control limits and the sampling frequency. The proposed hybrid adaptive schemes consider both variable sampling interval and variable sample size combined with run rules. The objective of this research is to develop a statistical comparison between adaptive schemes, charts with run rules and hybrid adaptive schemes with run rules to help decision-makers in the selection of the best performing chart for an expected value of shift in the mean of a controlled parameter. An extensive set of numerical results is presented to test the effectiveness of the proposed models in detecting small and moderate shifts in the process mean. The optimal statistical designs of the charts are obtained through a heuristic algorithm, properly modified to cope with the problem.

Keywords Adaptive schemes · Average time to signal · Control charts · Optimisation · Run rules

1 Introduction

Nowadays, strong competition among industries, due to a global market that considers customer satisfaction as a primary objective, requires high-quality and efficient products to be manufactured. Statistical process control (SPC) is a key approach to achieve rational management of manufacturing processes that allows final products, characterised by high quality, to be produced. Shewhart control charts are one of the most powerful tools in SPC; they are easy to implement and allow the statistical control state of a critical parameter in a manufacturing process to be checked and plotted. These control charts are designed by selecting the sample size n, the width of control limits k and sampling frequency t. A statistical limit of these control charts is represented by their poor sensitivity in the detection of out-of-control conditions when small shifts in the mean of the controlled parameters occur. A possible way to improve the statistical behaviour of the chart could be to restrict the control interval, but this solution results in an excessive amount of false alarms, which causes too large a number of operator interventions. For this reason, many authors have proposed models of Shewhart control charts that modify the original scheme and allow the statistical properties of these charts to be improved. Traditionally, two main approaches have been investigated by the researchers: the adaptive schemes, which permit the sample size and sampling interval to be changed, and the run rules – that is, the introduction of warning zones within the control interval of the chart, which calls for an action not only when a point falls outside the control limits, but also when a sequence of points falling within a warning zone verify a particular rule.

The former approach has been widely investigated in literature for different kinds of control charts; Tagaras [1] presented a complete survey of the developments in the design of several adaptive charts; variable sampling interval (VSI) control charts have been investigated by Reynolds et al. [2], Runger and Pignatiello [3], Runger and Montgomery [4], Reynolds [5]; the economic design of VSI control charts has been proposed by Das et al. [6], who compared the costs of the system when VSI and traditional control charts are implemented. The obtained results show that the cost savings obtained through a VSI approach with respect to the traditional scheme decreases when large shifts in the mean of the controlled parameter are considered.

Variable sample size control charts schemes (VSS) have been proposed by Prabhu et al. [7], who considered several shift sizes and measured their effectiveness through an Avaerage Run Length (ARL) evaluation. Costa [8] investigated the efficiency of the VSS charts through a comparison with several other control chart schemes, including an Exponentially Weighted Moving

G. Celano (✉) · A. Costa · S. Fichera
Dipartimento di Ingegneria Industriale e Meccanica,
University of Catania,
Viale Andrea Doria 6, 95125 Catania, Italy
E-mail: gcelano@diim.unict.it
Tel.: +39-0957382423
Fax: +39-095377994

Average (EWMA) chart, a Cumulative Sum (CUSUM) control chart and a standard $\bar{X}$ chart with run rules. Zimmer et al. [9] evaluated the effectiveness of three-state adaptive schemes and demonstrated that the simpler two-state scheme works as well.

Combined adaptive control charts (VSSI) with variable sample size and variable sampling interval were also developed and tested. Prabhu et al. [10] proposed several examples to demonstrate the improvements obtained through the VSSI scheme; they also determined optimal values for the maximum sample size and studied a case from an industrial process to test their model. Costa [11] compared the performances of the VSSI adaptive scheme with Shewhart charts with and without run rules, and combined Shewhart-CUSUM and EWMA schemes when the assignable cause does not occur at the beginning of the process but during the production time. The parameter used for the comparison is the adjusted average time to signal, (AATS) and the occurrence of a shift in the mean of the controlled parameter is modelled as an exponentially distributed random variable. The economic statistical design of VSSI $\bar{X}$ control charts was developed and compared to a traditional Shewhart scheme by Prabhu et al. [12]. The charts have been compared in terms of cost of operation and average time to signal.

Control charts with run rules allow the statistical performance of the $\bar{X}$ chart to be improved through a set of warning limits acting within the control interval of the chart itself [13]. The width of the warning zones can be determined with respect to a statistical or an economic objective. Parkhideh and Parkhideh [14] adapted the economic design of a Shewhart $\bar{X}$ chart to the improved scheme with run rules, (Western Electric rules $C1$, $C2$ and $C3$) and showed how the introduction of the warning zones allows a reduction in the expected costs to be reached. Parkhideh and Parkhideh [15] analysed the statistical performances of a flexible zone control chart for individual measurements with respect to a traditional Shewhart $\bar{X}$ chart; the optimisation of the statistical performances was obtained for both rules $C1$ and $C2$, (C_{12}), as well as rules $C1$, $C2$ and $C3$, (C_{123}).

Adaptive control charts with run rules were developed to take into account the past history of the process, in order to improve the chart capability in detecting out-of-control conditions. Run rules were added by Reynolds et al. [2] to a VSI adaptive scheme to manage the presence of out-of-control conditions in the process; the selected run rules considered r' out of r sample means falling within the warning zones of the chart or a point falling outside the control limits as out-of-control signals: they developed a set of examples where a VSI chart with run rules considering $r' = 2$ out of $r = 3$ (called rule 1) and $r' = 5$ out of $r = 5$ (five consecutive points, called rule 2) was compared with a traditional Shewhart chart with the same run rules. They compared the two charts on the basis of the AATS, (the in-control AATS = ATS(0) should be the same for the different charts), which was evaluated through the Markov chain approach proposed by Champ and Woodall [16]. A similar approach was followed by Reynolds [5] to improve the statistical performance of a variable sampling interval control chart with sampling at fixed times (VSIFT).

Run rules were also introduced as switching rules in the selection of the sampling interval by Amin and Letsinger [17] and Amin and Hemashina [18]. Here, the length of the sampling interval is a function of the last r plotted points on the chart: if r' out of r last plotted sample means fall within the warning zones, the sampling interval is reduced to t_1; otherwise, it is maintained such that $t_2 > t_1$. In this way, the number of switches between the different sampling intervals is reduced.

Cui and Reynolds [19] developed VSI $\bar{X}$ control charts where run rules work on both the signalling and switching procedure from one sampling interval to another. In this model, sequences of consecutive points are considered to decide if the process is in an out-of-control condition or which sampling interval must be selected to plot the following point in the chart. The results show how the improved performance in AATS with respect to a static chart is due to the run rules when small shifts are considered and due to the VSI scheme for larger shifts. The economic design of the Cui and Reynolds [19] $\bar{X}$ chart was performed by Das et al. [6].

Even if several papers dealing with the statistical properties of a variable sampling interval $\bar{X}$ chart with run rules were investigated in literature, no research was devoted to the rule application to variable sample size (VSS) and combined variable sample size and interval (VSSI) schemes. Tagaras [1] does not mention any paper dealing with such models. For this reason, in this paper, the statistical properties of VSS and VSSI $\bar{X}$ charts with run rules are investigated and compared with other existing models. Here, the rules are introduced only as signalling tools of an out-of-control condition; the selection of sampling intervals and sample sizes depends only on the position of the last plotted point on the chart. The AATS, when the process is out of control, is the statistical performance parameter used to compare the ability of the proposed schemes in the detection of the process shift from $\mu = \mu_0$ to $\mu = \mu_1$. The optimal statistical designs of the chart have been determined through a heuristic algorithm; namely, simulated annealing, operating on a function which depends on the AATS with process in "in-control" and "out-of-control" conditions and considering a specific set of constraints acting to make possible the comparison between the different chart schemes.

The rest of the paper is organised as follows: in the next section, the formulation of the proposed charts without and with run rules is developed; then, the optimising heuristic procedure is presented; finally, the obtained results are reported and discussed.

2 Description of the developed charts

The developed adaptive $\bar{X}$ control charts have been investigated by assuming as a statistical performance index the adjusted average time to signal (AATS). This performance measure represents the expected time interval between the occurrence of an assignable cause and the time the charts signal an out-of-control condition. The AATS is computed with respect to the steady state performance of the chart, i.e. assuming a process evolution

characterised by a start in the "in-control" condition and a successive shift occurring at some random time in the future. The shift in the mean μ_0 of the controlled parameter is expressed as a multiple of the population standard deviation σ; that is, assuming $\mu_1 = \mu_0 + \delta\sigma$. The different adaptive schemes have been statistically compared through the evaluation of their AATS corresponding to different values of the shift under the following constraints: equal in-control ATS(0), expected sample size n_0 and sampling interval t_0. The following notation is adopted in the rest of the paper:

n_1, n_2: smaller and larger sample size;
t_1, t_2: smaller and larger sampling interval;
n_0: expected sample size when the process is "in-control";
t_0: expected sampling interval when the process is "in-control";
k, w, l: width of control and threshold limits;
μ_0: mean of the controlled parameter when the process is "in-control";
μ_1: mean of the controlled parameter when the process is "out-of-control";
σ: standard deviation of the controlled parameter;
δ: shift in the mean of the controlled parameter;
$ARL(0)$: chart average run length when the process is "in-control", i.e. the average number of samples to be taken between two successive false alarms;
$ARL(\delta)$: chart average run length when the process is "out-of-control", i.e. average number of samples to be taken between the occurrence of the special cause and the signal;
$ATS(0)$: chart average time to signal when the process is "in-control", i.e. average elapsed time between two successive false alarms;
$AATS(\delta)$: chart adjusted average time to signal when the process is "out-of-control", i.e. average elapsed time between the occurrence of the special cause and the signal;

2.1 Adaptive charts without run rules

The classical two-state adaptive charts have been investigated in this paper. The schemes have been developed by considering the standardised mean:

$$Z = \frac{\bar{X} - \mu_0}{\sigma_{\bar{X}}} \tag{1}$$

The control limits of the standardised charts, denoted as the upper control limit (UCL) and lower control limit (LCL) are positioned at $\pm k$ apart from 0. The threshold limits are positioned at $\pm w$ apart from 0, where $w < k$ (see Fig. 1).

In particular, for the adaptive sampling interval VSI scheme, the following function was adopted:

$$t = \begin{cases} t_1 & \text{if } -k < Z < -w \\ t_2 & \text{if } -w < Z < w \\ t_1 & \text{if } w < Z < k \end{cases} \tag{2}$$

where t_1 represents the shorter sampling interval, and t_2 is the larger sampling interval. The sample size is constant and equal to n_0.

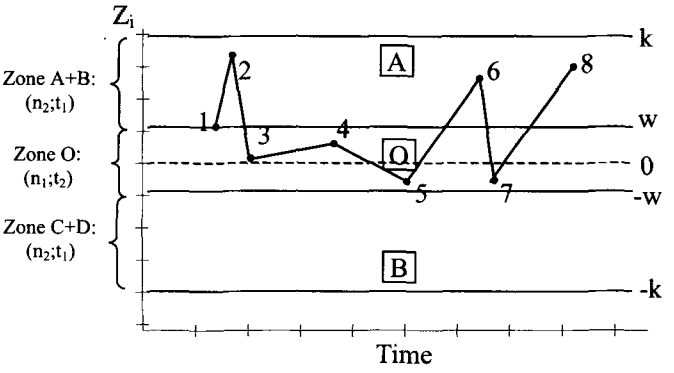

Fig. 1. The VSSI adaptive scheme without run rules

The adaptive sample size VSS scheme was formalised through the following function:

$$n = \begin{cases} n_2 & \text{if } -k < Z < -w \\ n_1 & \text{if } -w < Z < w \\ n_2 & \text{if } w < Z < k \end{cases} \tag{3}$$

where n_1 is the smaller sample size and n_2 is the larger sample size. The sampling interval is constant and equal to t_0.

The combined adaptive sample size and interval VSSI scheme was formulated considering the following expression:

$$n, t = \begin{cases} n_2, t_1 & \text{if } -k < Z < -w \\ n_1, t_2 & \text{if } -w < Z < w \\ n_2, t_1 & \text{if } w < Z < k \end{cases} \tag{4}$$

The Markov chain approach proposed in Zimmer et al. [9] was considered to evaluate the in-control and out-of-control ARLs, $ARL(0)$ and $ARL(\delta)$, corresponding to the developed adaptive schemes reported above:

$$ARL(0) = \boldsymbol{b}'\left(\boldsymbol{I} - \boldsymbol{Q}^0\right)^{-1} \cdot \mathbf{1}$$
$$ARL(\delta) = \boldsymbol{b}'\left(\boldsymbol{I} - \boldsymbol{Q}^\delta\right)^{-1} \cdot \mathbf{1} \tag{5}$$

where $\delta \geq 0$. $\boldsymbol{b}'(1 \times 2)$ represents the vector of initial probabilities corresponding to steady-state performance, $\boldsymbol{I}(2 \times 2)$ is the identity matrix, and $\boldsymbol{Q}(2 \times 2)$ is the state transition matrix of the Markov chain. Therefore, $\boldsymbol{Q}^0$ and $\boldsymbol{Q}^\delta$ are the state transition matrices for an in-control and out-of-control process, respectively. Similarly, the in-control ATS is computed using the following expression:

$$ATS(0) = \boldsymbol{b}'\left(\boldsymbol{I} - \boldsymbol{Q}^0\right)^{-1} \cdot \boldsymbol{t} \tag{6}$$

$\boldsymbol{t}'$ is the vector of sampling intervals. For more details about the evaluation of Eqs. 5 and 6, see Zimmer et al. [9]. The out-of-control $ATS(\delta)$ evaluated here considers a process that starts in the in-control state and then shifts to the out-of-control condition after a generic time interval; therefore, the steady-state perform-

ance of the chart must be considered, and the $ATS(\delta)$ coincides with the adjusted average time to signal $AATS(\delta)$ [1, 3]:

$$AATS(\delta) = E(Y) + E(t_i) \cdot (ARL(\delta) - 1) \tag{7}$$

where $E(Y)$ is the time elapsed between the occurrence of the process shift and the next sample; $E(t_i)$ is the expected length of sampling frequency when the process is in an out-of-control condition. In this way, it is possible to determine the $AATS(\delta)$ through the following expression:

$$\begin{aligned} AATS(\delta) = &\left[\left(\frac{t_2}{2}\right) \cdot \frac{\Phi(w) - \Phi(-w)}{\Phi(k) - \Phi(-k)} \cdot \frac{t_2}{t_0}\right. \\ &\left. + \left(\frac{t_1}{2}\right) \cdot \frac{2 \cdot (\Phi(k) - \Phi(w))}{\Phi(k) - \Phi(-k)} \cdot \frac{t_1}{t_0}\right] \\ &- t_0 + \{b'\} \cdot [I - Q^{\delta}]^{-1} \cdot \{t\} \end{aligned} \tag{8}$$

This equation coincides numerically with that proposed by Das et al. [6] for the VSI chart when the special cause is assumed to occur in the middle of a sampling interval, whose expected length is equal to $t_0/2$.

2.2 Adaptive charts with run rules

Run rules are added to control charts to improve their statistical performance when small shifts in the mean of the controlled parameter are expected. The rules have been implemented in Shewhart control charts to detect possible shifts in the mean of the controlled parameter. Rules considering both consecutive and non-consecutive points have been developed by the researchers. For traditional Shewhart control charts, run rules that give an out-of-control signal when r of the last m plotted points fall within the interval (a, b) were considered by Champ and Woodall [16] and Parkhideh and Parkhideh [15]. They are usually denoted by $T(r, m, a, b)$. Following the notation proposed in Champ and Woodall [16], the following rules have been considered in this paper:

$$\begin{aligned} C1 &= \{T(1, 1, -\infty, -k), T(1, 1, k, \infty)\} \\ C2 &= \{T(2, 3, -k, -w), T(2, 3, w, k)\} \\ C3 &= \{T(4, 5, -k, -l), T(4, 5, l, k)\} \end{aligned} \tag{9}$$

where $l < w < k$ are the threshold limits whose values are optimised with respect to the ATS. Rule $C1$ corresponds to the out-of-control condition of the standard Shewhart chart; rules $C2$ and $C3$ consider short sequences of non-consecutive points to signal a possible out-of-control condition. The rules can be combined to improve the statistical properties of the chart.

The $AATS(\delta)$ of Shewhart control charts with run rules can be computed as $t \cdot ARL(\delta)$, where t is the length of the sampling interval and the $ARL(\delta)$ is computed assuming that the process starts in the "in-control" condition, i.e. with a point falling in the internal zone of the chart control interval. A Markov chain approach based on the possible states of the process corresponding to the position of plotted points was proposed by Champ and Woodall [16] to compute the $ARL(\delta)$.

The $AATS(\delta)$ evaluation for adaptive charts with run rules needs the formulation of a Markov chain approach as well. Cui and Reynolds [19] and later, Das et al. [6], developed a Markov chain model for VSI schemes when consecutive points are monitored to select the sampling interval and to call for an out-of-control condition. In this research, a proper Markov chain model, based on the approach given by Artiles-Leon et al. [20], is developed; this depends on the possibility of considering non-consecutive points and varying the sample sizes. Due to these two assumptions, each possible state of the process must consider almost the last m plotted points and the corresponding selected sample sizes. The implemented run rules operate only to signal out-of-control conditions and not as a decision rule to select the sample size and/or the sampling interval. To explain the adopted Markov chain model, let us consider the adaptive VSSI scheme with run rules $C1$, $C2$ and $C3$ (VSSI123) reported in Fig. 2.

The standardised chart control interval is divided by the threshold limits into five warning zones: $A(w, k)$, $B(l, w)$, $O(-l, l)$, $C(-w, -l)$, and $D(-k, -w)$. A dual sample size and sampling interval policy is adopted:

$$n, t = \begin{cases} n_2, t_1 & \text{if } -k < Z < -l \\ n_1, t_2 & \text{if } -l < Z < l \\ n_2, t_1 & \text{if } l < Z < k \end{cases} \tag{10}$$

In the proposed scheme, the threshold limit l and the control limit k are used both for implementing the adaptive scheme and the run rules, whereas the threshold limit w works only on run rules. As an example, in Fig. 1, the points 7 and 9, falling within the $A(w, k)$ zone, signal for an out-of-control condition, in accordance with run rule $C2$. As threshold limit of the adaptive scheme l was selected instead of w to improve the statistical effects of the chart; this allows the selection of the couple (n_2, t_1) to be extended to a wider portion of the control interval than with w as adaptive policy threshold limit. The same limits for an adaptive scheme and run rules were selected in order to simplify the chart interpretation and construction.

The developed Markov chain model requires the position of the last m plotted points on the chart to list all of the possible states characterising the process. Considering the VSSI123

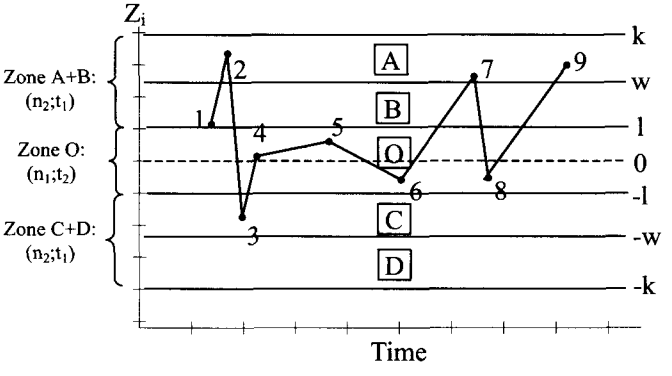

Fig. 2. The hybrid VSSI adaptive scheme with run rules $C1$, $C2$ and $C3$ (VSSI123)

scheme, the five mentioned warning zones and the last $m = 4$ plotted points must be considered to determine the set of non-absorbing states of the chain. By denoting a plotted point, i.e. a standardised mean Z_i, falling within a warning zone with the corresponding zone identifier, (A, B, C, D, or O), the generic state of the process can be represented with a four-letter vector [X X X X]. For example, four consecutive points falling within zone O constitute a possible state denoted as [O O O O]; similarly, in Fig. 1 points 1–4 correspond to [B A C O]. With consideration of this notation, it is possible to determine the entire set of non-absorbing states of the chain for the VSSI scheme with run rules $C1$, $C2$ and $C3$, (C_{123} scheme). Denoting as S the complete space state, the total number of states $|S|$, including absorbing and non-absorbing ones, is equal to N^r, where N is the number of warning zones and r the length of the sequence of consecutive points. For the VSSI123 scheme, $|S| = 5^4 = 625$. The absorbing states are those including one point falling out of control limits (rule $C1$), two out of three points falling within zones A or D (rule $C2$), and four out of five points falling within zones A and/or B or, alternatively, zones C and D (rule $C3$). As an example, [A O A O] is an absorbing state with respect to rule $C2$ and [A B A B] leads to absorption due to rule $C3$. Once the state space dimension has been fixed, it is possible to determine the state transition matrix $\boldsymbol{P}$, whose dimension is 625×625. Each element of this matrix represents the probability of transition from one state to another. Eliminating the absorbing states from the state space, the cardinality of S is reduced to $|S^*| = 423$. As a consequence, the non-absorbing state transition matrix $\boldsymbol{Q}$ can be obtained from $\boldsymbol{P}$ by deleting the rows and columns corresponding to absorbing states; therefore, $\boldsymbol{Q}$ has dimension 423×423:

$$\boldsymbol{Q} = \begin{array}{c|cccc} & OOOO & OOOA & \ldots\ \ldots & DCOD \\ OOOO & p_O & p_A & & 0 \\ OOOA & 0 & 0 & & 0 \\ \ldots & & & \ldots & \\ \ldots & & & \ldots & \\ DCOD & 0 & 0 & & 0 \end{array} \tag{11}$$

The elements of this matrix equal to 0 correspond to non-allowable one-step transitions ([$OOOO$] $\rightarrow$ [$DCOD$]), or to transitions to absorbing conditions ([$C\underline{C}O\underline{C}$] $\rightarrow$ [$\underline{C}O\underline{C}C$], i.e. four of the last five plotted points fall within zone C). The elements of matrix $\boldsymbol{Q}$ not equal to 0 correspond to the probability of a point falling within a warning zone of the chart control interval. This probability is a function of k, w and l when the process works in an "in-control" condition and also of δ, n_1, n_2, when the process operates in an "out-of-control" condition. Therefore, by denoting as $\boldsymbol{Q}^0$ the "in-control" non-absorbing state transition matrix, the expressions of the transition probabilities are:

$$\begin{aligned} p_A^0 &= \Phi(k) - \Phi(w) \\ p_B^0 &= \Phi(w) - \Phi(l) \\ p_O^0 &= \Phi(l) - \Phi(-l) \\ p_C^0 &= \Phi(-l) - \Phi(-w) \\ p_D^0 &= \Phi(-w) - \Phi(-k) \end{aligned} \tag{12}$$

whereas, in the "out-of-control" condition, by denoting as $\boldsymbol{Q}^\delta$ the "out-of-control" non-absorbing state transition matrix, the transition probabilities are evaluated through the following expressions:

$$\begin{aligned} p_A^\delta &= \Phi(k - \delta\sqrt{n_i}) - \Phi(w - \delta\sqrt{n_i}) \\ p_B^\delta &= \Phi(w - \delta\sqrt{n_i}) - \Phi(l - \delta\sqrt{n_i}) \\ p_O^\delta &= \Phi(l - \delta\sqrt{n_i}) - \Phi(-l - \delta\sqrt{n_i}) \\ p_C^\delta &= \Phi(-l - \delta\sqrt{n_i}) - \Phi(-w - \delta\sqrt{n_i}) \\ p_D^\delta &= \Phi(-w - \delta\sqrt{n_i}) - \Phi(-k - \delta\sqrt{n_i}) \end{aligned} \tag{13}$$

where δ is connected to the entity of the shift in the mean of the controlled parameter through the expression $\mu_1 = \mu_0 + \delta\sigma$. The values of n_i ($i = 1,2$) to be introduced within the above expressions depend on the position of the last plotted point on the chart. If this point falls within zones $A + B$ or $C + D$, i.e. considering transitions from states characterised by A, B, C, or D as final point, $n_2 > n_1$ must be considered; otherwise, when transition probabilities from states characterised by a final point labelled as O are evaluated, it must be selected such that $n_i = n_1$. The consequence of this assumption is that two standardised shifts, $\Delta_1 = \delta\sqrt{n_1}$ and $\Delta_2 = \delta\sqrt{n_2}$, must be defined. As stated before, the comparison between the different charts' statistical performances is carried out assuming the same "in-control" $ATS(0)$, "in-control" expected sample size n_0 and sampling interval t_0. The evaluation of these quantities requires the definition of two subsets of non-absorbing states S' and S'' such that $S' + S'' = S$. Subset S' includes all of the states characterised by O as the final point. A successive point to one of them is plotted considering the lower sample size n_1 and the larger sampling interval t_2. Subset S'' includes all of the states characterised by A, B, C, or D as the final point: a successive point to one of them is plotted considering the upper sample size n_2 and the shorter sampling interval t_1. Therefore, n_0 and t_0 are computed respectively as:

$$n_0 = \sum_{j \in S'} \pi_j n_1 + \sum_{k \in S''} \pi_k n_2 \tag{14}$$

$$t_0 = \sum_{j \in S'} \pi_j t_2 + \sum_{k \in S''} \pi_k t_1 \tag{15}$$

where π_i, ($i = 1, \ldots, |S^*|$), are the steady-state probabilities with an "in-control" process condition:

$$\begin{aligned} &\boldsymbol{\pi} = \boldsymbol{\pi} \times \boldsymbol{Q}^0 \\ &\sum_{i=1}^{|S^*|} \pi_i = 1 \end{aligned} \tag{16}$$

The "in-control" $ATS(0)$ is computed assuming that the process starts in the "in-control" condition in the state [O O O O]; as a consequence, the average time to signal before a false alarm is equal to the first element of the vector

$$\begin{aligned} &\{E(T)\}^0 = [\boldsymbol{I} - \boldsymbol{Q}^0]^{-1} \times \{t\}^T \\ &ATS(0) = E(T)_1^0 \end{aligned} \tag{17}$$

The $AATS(\delta)$ is computed in the same way as for simple adaptive schemes – by introducing the summations of the steady-state probabilities with the process "in control" and, similarly to the $ATS(0)$ computation, referring to $[O\ O\ O\ O]$ as the initial state of the Markov chain:

$$AATS(\delta) = \left[\left(\frac{t_2}{2}\right)\cdot\sum_{j\in S'}\pi_j\cdot\frac{t_2}{t_0} + \left(\frac{t_1}{2}\right)\cdot\sum_{k\in S''}\pi_k\cdot\frac{t_1}{t_0}\right] - t_0 + ATS(\delta)$$

$$ATS(\delta) = E(T)_1^{\delta} \tag{18}$$

3 The optimisation procedure

The statistical designs of the charts were achieved by running a heuristic algorithm; namely, simulated annealing (SA). The algorithm was coded in FORTRAN and its structure refers to the one proposed by Kirkpatrick [21]. The efficiency of the proposed optimisation method in determining optimal designs for adaptive control charts was tested in a previous paper, Campisi et al. [22], where a comparison with other numerical methods was carried out to economically design both static and adaptive control charts. The SA algorithms operate through an analogy to statistical mechanics of condensed matter physics. They represent an enhanced version of the traditional techniques of local optimisation or iterative improvement and allow the probability of accepting poor local optimal solutions to be reduced. The latter issue is possible since SA gives the possibility to probabilistically accepting "retrogressive" movements towards worse solutions, thus allowing new possible optimal solutions to be found.

The variables needed to define the statistical design of the chart are grouped within a design vector $\boldsymbol{D}$, whose length depends on the selected chart to be designed (see Table 1).

The objective function $OBJ(\boldsymbol{D})$ corresponding to each sequence $\boldsymbol{D}$ was formulated assuming that a feasible design must respect the constraints relative to in-control $ATS(0)$, ($ATS(0)$ equal to an $ATS(0)^*$ properly selected by the decision-maker) and on n_0 and t_0. All of the compared charts must be characterised by the same expected sample size and interval. Therefore, the following function $OBJ(\boldsymbol{D})$ was adopted:

$$OBJ(\boldsymbol{D}) = \begin{cases} |ATS(0) - ATS(0)^*| + AATS(\delta) \\ \qquad \text{if } |ATS(0) - ATS(0)^*| < \varepsilon \quad \varepsilon \in (0.5;\ 1) \\ 10\cdot(|ATS(0) - ATS(0)^*| + AATS(\delta)) \\ \qquad \text{if } |ATS(0) - ATS(0)^*| > \varepsilon \end{cases} \tag{19}$$

The constraints on n_0 and t_0 are respected by entire set of investigated solutions when the static and adaptive chart schemes without rules are optimised. In fact, as shown in Table 1, some variables of the problem are determined as a function of the others assuming $E(n) = n_0$ and $E(t) = t_0$. For further details, see Prabhu et al. [12] and Zimmer et al. [9]. When schemes with run rules are adopted, the design optimisation is more complicated, due to an higher number of variables and difficulty in explaining a set of equations corresponding to the selected constraints; therefore, the search of the optimal design is performed by following three successive stages: first of all, a subset of $\boldsymbol{D}$ including feasible control and threshold limits k', w' and l' is determined within the space of solutions, which respects the following constraint:

$$|ARL(k', w', l') - ATS(0)^*/t_0| < \varepsilon' \quad \varepsilon' \in (0;\ 0.5) \tag{20}$$

where $ATS(0)^*$ and t_0 are fixed a priori. Once a candidate triple of limits has been identified, the heuristic search is focused on the sampling intervals t_1 and t_2 (VSI and VSSI schemes); in the whole set of possible intervals, a candidate couple is selected, which satisfies

$$|ATS(0)[k', w', l', t_1', t_2'] - ATS0^*| < \varepsilon'' \quad \varepsilon'' \in (0;\ 0.5) \tag{21}$$

Finally, the sample sizes n_1 and n_2 (VSS and VSSI schemes) are investigated in order to verify the constraint on expected sample size:

$$\left|\sum_{j\in S'}\pi_j(k', w', l')n_1' + \sum_{k\in S''}\pi_k(k', w', l')n_2' - n_0\right| < \varepsilon'''$$

$$\varepsilon''' \in (0;\ 0.5) \tag{22}$$

where n_0 is fixed a priori. At the end of the three-stage procedure, a feasible design of the chart respecting all of the constraints is assumed as an actual sequence $\boldsymbol{D}$ of the simulated annealing and the search is continued by perturbing $\boldsymbol{D}$ and trying to determine better feasible solutions.

Table 1. The sequences optimised by the SA to design the investigated charts

Shewhart	Simple	$\boldsymbol{D} = \{n, k, t\}$
	C_{12}	$\boldsymbol{D} = \{n, k, w, t\}$
	C_{123}	$\boldsymbol{D} = \{n, k, w, l, t\}$
VSS	Simple	$\boldsymbol{D} = \{n_1, n_2, k, t\}$ with $n_1 < n_2$ and $w = w(k, n_1, n_2)$ calculated
	C_{12} (VSS12)	$\boldsymbol{D} = \{n_1, n_2, k, w, t\}$ with $n_1 < n_2$
	C_{123} (VSS123)	$\boldsymbol{D} = \{n_1, n_2, k, w, l, t\}$ with $n_1 < n_2$
VSI	Simple	$\boldsymbol{D} = \{n, k, t_1, t_2\}$ with $t_1 < t_2$ and $w = w(k, t_1, t_2)$ calculated
	C_{12} (VSI12)	$\boldsymbol{D} = \{n, k, w, t_1, t_2\}$ with $t_1 < t_2$
	C_{123} (VSI123)	$\boldsymbol{D} = \{n, k, w, l, t_1, t_2\}$ with $t_1 < t_2$
VSSI	Simple	$\boldsymbol{D} = \{n_1, n_2, k, t_1\}$ with $n_1 < n_2$ and $t_1 < t_2$, $w = w(k, n_1, n_2)$ and t_2 calculated
	C_{12} (VSSI12)	$\boldsymbol{D} = \{n_1, n_2, k, w, t_1, t_2\}$ with $n_1 < n_2$ and $t_1 < t_2$
	C_{123} (VSSI123)	$\boldsymbol{D} = \{n_1, n_2, k, w, l, t_1, t_2\}$ with $n_1 < n_2$ and $t_1 < t_2$

The SA investigates the space of allowable solutions through a neighbourhood search scheme, which modifies the actual sequence $\boldsymbol{D}$ to the perturbed $\boldsymbol{D}'$ by randomly varying one or more elements of $\boldsymbol{D}$ and recalculating the dependent variables through the three-stage procedure in order to respect the fixed constraints.

The SA algorithm evolves through a series of levels, called "temperatures". A cooling schedule based on the variation of the objective function $OBJ(\boldsymbol{D})$ and on the actual temperature stage has been chosen, Kirkpatrick [21]. At each temperature stage T_i, a local search is performed in the neighbourhood of the current sequence according to a "last improvement-basis" scheme: the current sequence is perturbed according to the neighbourhood search scheme proposed above. If the newly evaluated vector $\boldsymbol{D}'$ has an objective function whose value is lower than the one corresponding to the original vector $\boldsymbol{D}$, it is accepted and becomes the new actual sequence.

On the other hand, if the vector $\boldsymbol{D}'$ has a worse value of $OBJ(\boldsymbol{D}')$, it is accepted only if the following expression is verified:

$$\text{rand}(x) < \exp\{-[OBJ(\boldsymbol{D}') - OBJ(\boldsymbol{D})]/T\} \tag{23}$$

where $\text{rand}(x) \in [0, 1]$. Therefore, the probabilistic acceptance of a worse sequence strongly depends on the counteraction between variation in the objective function and the actual temperature stage.

The cardinality *maxiter* of the neighbourhood in the local search at each temperature level depends on the problem size; that is, on the length of vector $\boldsymbol{D}$. The last accepted sequence during the local search will be the actual sequence in the successive temperature stage. A low value of T_i has been chosen in order to reach a good compromise ratio between the analysed and the worst accepted sequences. The algorithm is judged to be frozen when the temperature reaches a final value T_f. When adaptive schemes with run rules are investigated, the high computational effort due to the three-stage procedure and the dimensions of transition probability matrices require a shortened SA evolution with a reduced initial temperature and a low value of *maxiter*. The procedure of the modified SA algorithm for the adaptive charts with run rules is proposed below:

Step 1: Initialise: T_i, α, *maxiter* and $iter = 1$. Read the input data of the problem: $ATS0^*$, t_0 and n_0.
Step 2: Randomly create a feasible seed sequence and assign it to the $\boldsymbol{D}$ and $\boldsymbol{MEM}$ vectors.
Step 3: Evaluate the $OBJ(\boldsymbol{D})$ value for $\boldsymbol{D}$ and assign it to the variable $\boldsymbol{BEST}$.
Step 4: Generate the perturbed sequence $\boldsymbol{D}'$ with the neighbourhood operator following the three-stage procedure, $iter = iter + 1$.
Step 5: Evaluate the $OBJ(\boldsymbol{D}')$ value for $\boldsymbol{D}'$.
Step 6: If $OBJ(\boldsymbol{D}') < BEST$, then
let $\boldsymbol{D} = \boldsymbol{D}'$, $\boldsymbol{MEM} = \boldsymbol{D}'$. Go to Step 11.
Step 7: Evaluate $\Delta = OBJ(\boldsymbol{D}') - OBJ(\boldsymbol{D})$.
Step 8: If $\Delta < 0$, then
let $\boldsymbol{D} = \boldsymbol{D}'$. Go to Step 11.
Step 9: Generate a random number x.
Step 10: If $f(x) < \exp(-\Delta/T)$, then
let $\boldsymbol{D} = \boldsymbol{D}'$.
Step 11: If $iter < maxiter$ then
Go to step 4
else
let $T = \alpha T$ and $iter = 1$.
Step 12: If $T > T_f$, then go to Step 4.
Step 13: STOP. Best chart design memorised in $\boldsymbol{MEM}$.

4 Computational results

The statistical performances of the investigated charts have been compared by taking into account different levels of in-control $ATS(0)$, expected sample sizes $E(n) = n_0$ and expected sampling interval $E(t) = t_0$. In contrast to previous literature [10, 23], no specific values were imposed on the shorter sampling interval or on the sample size; thus, a fully optimised statistical design can be achieved. However, a partial optimisation with fixed values for a subset of design variables can be easily obtained through the proposed SA algorithm by fixing a priori one or more of the elements of the array $\boldsymbol{D}$. The following constraints have been considered to test the charts statistical performances: two levels for in-control ATS(0): $ATS(0)^* = 370.4$ and 499.6; three levels for the expected sample size $E(n) = n_0 = 3, 5, 10$ and one level for the expected sampling interval $E(t) = t_0 = 1$. As stated above, the adopted run rules are $C1$, $C2$ and $C3$ (see Eq. 9). The sample size can range within the interval [1,30], whereas the sampling interval within [0.1,2]. The statistical design was determined for a wide range of process mean shifts between 0 and 2.25. Tables 2–7 show the obtained results, grouped with reference to the value of in-control $ATS(0)$ and expected sample size n_0. The statistical designs corresponding to the lowest $AATS(\delta)$ are reported with a bolded italic notation. From the results, it can be noted that the VSSI scheme with rules $C1$, $C2$ and $C3$ (VSSI123) always outperforms the other charts when small shifts are expected in the mean of the controlled parameter; that is, when $\delta < 0.6$. Assuming $ATS(0)^* = 370.4$ and $n_0 = 3$, a maximum reduction of $AATS(\delta)$ between simple VSSI and VSSI123 equal to approximately 50% can be achieved; this reduction increases to 55% and to 62% when $n_0 = 5, 10$, respectively. When $ATS(0)^* = 499.6$ is selected as in-control ATS, the gap goes up to 51%, 59% and 65% for $n_0 = 3, 5, 10$, respectively. The same trend can be noted for VSI123 and VSS123. Thus, the larger the $ATS(0)$ and expected sample size, the larger the statistical performance improvement of the adaptive scheme with run rules with respect to a simple adaptive scheme. As expected, when the entity of the shift is moderate to large, the performances of adaptive schemes with run rules slightly deteriorate due to the run rules; however, their $AATS(\delta)$ still remains quite similar to that of the other charts. This fact can be easily explained by comparing Shewhart charts with run rules and simple adaptive schemes. The run rules outperform the adaptive schemes only when very small shifts ($\delta < 0.3$) occur to the mean of the controlled parameter, whereas the adaptive schemes are particularly suited for moderate to large deviations. The positive effect of run rules is

Table 2. Comparison among the optimal $AATS(\delta)$ corresponding to the charts: $ATS(0) = 370.4$, $n_0 = 3$, $t_0 = 1$

	δ																
	0	0.1	0.15	0.2	0.25	0.3	0.35	0.4	0.5	0.6	0.75	1	1.25	1.5	1.75	2	2.25
								No rules (C_1)									
Shewhart	370.40	321.60	275.16	227.22	183.74	147.03	117.24	93.54	60.19	39.53	21.98	9.26	4.45	2.41	1.45	0.97	0.73
VSS	370.40	316.35	254.38	184.03	121.09	75.04	45.90	28.99	14.46	9.46	5.58	3.06	1.99	1.60	1.31	0.97	0.92
VSI	370.40	318.43	268.77	217.79	171.74	132.83	101.92	77.96	45.86	26.85	12.94	4.35	1.86	1.85	0.89	0.83	0.67
VSSI	370.40	314.91	252.85	181.22	117.85	72.27	43.58	27.50	13.93	**7.91**	**4.69**	**2.82**	**1.60**	1.46	**0.83**	0.97	0.73
								Rules $C1$, $C2$ (C_{12})									
Shewhart	370.40	290.98	227.90	172.23	128.61	96.17	72.49	54.87	32.72	20.64	11.32	5.13	2.87	1.87	1.35	1.04	0.83
VSS	370.40	237.37	157.43	102.49	70.18	47.04	32.51	23.42	13.56	9.01	5.80	3.68	2.71	2.06	1.61	1.32	1.09
VSI	370.40	289.31	225.20	170.41	126.53	92.60	70.04	52.73	31.10	23.63	12.31	4.98	2.45	**1.41**	0.94	**0.71**	**0.60**
VSSI	370.40	236.82	157.19	103.21	68.28	45.66	32.66	23.37	13.23	8.76	5.27	2.96	1.92	1.56	1.14	0.89	0.73
								Rules $C1$, $C2$, $C3$ (C_{123})									
Shewhart	370.40	258.61	184.93	129.61	91.55	65.92	48.57	36.63	22.31	14.76	9.05	5.22	3.70	2.83	2.17	1.65	1.27
VSS	370.40	219.96	142.31	92.61	62.21	43.36	31.34	23.45	14.41	9.84	6.48	4.21	3.12	2.43	1.99	1.74	1.61
VSI	370.40	256.77	181.93	125.89	87.53	61.85	44.61	32.87	19.00	11.87	6.65	3.29	2.06	1.53	1.29	1.18	1.12
VSSI	370.40	**218.56**	**140.24**	**90.24**	**59.74**	**40.92**	**29.01**	**21.23**	**12.41**	8.02	4.87	2.91	2.21	1.83	1.59	1.42	1.31

Table 3. Comparison among the optimal $AATS(\delta)$ corresponding to the charts: $ATS(0) = 370.4$, $n_0 = 5$, $t_0 = 1$

	δ																
	0	0.1	0.15	0.2	0.25	0.3	0.35	0.4	0.5	0.6	0.75	1	1.25	1.5	1.75	2	2.25
								No rules (C_1)									
Shewhart	370.40	295.25	233.15	177.23	132.66	99.05	74.26	56.09	32.90	20.06	10.26	4.00	1.89	1.07	0.72	0.58	0.52
VSS	370.40	285.85	204.08	128.40	74.46	42.11	24.48	15.94	7.91	5.30	3.68	1.92	1.34	0.97	0.80	0.65	0.56
VSI	370.40	290.22	223.94	164.70	117.89	83.71	59.58	41.87	21.87	11.56	4.89	1.90	0.97	0.89	0.66	0.57	0.53
VSSI	370.40	283.06	199.74	123.41	69.81	38.05	21.56	12.87	**6.73**	**3.90**	**2.50**	**1.28**	**0.85**	0.79	0.71	0.65	0.62
								Rules $C1$, $C2$ (C_{12})									
Shewhart	370.40	253.97	178.65	122.58	84.46	59.15	42.30	30.54	17.01	10.36	5.60	2.65	1.60	1.11	0.82	0.65	0.55
VSS	370.40	206.46	125.91	77.50	48.98	32.24	22.16	15.50	8.54	5.50	3.49	2.24	1.88	1.06	0.72	0.57	0.52
VSI	370.40	251.38	177.12	120.48	81.07	56.93	40.42	28.99	19.21	11.15	5.52	2.22	1.15	**0.75**	**0.59**	**0.53**	**0.51**
VSSI	370.40	206.38	125.55	76.69	48.22	30.95	21.03	14.52	7.76	4.82	2.85	1.67	1.04	0.78	0.65	0.58	0.55
								Rules $C1$, $C2$, $C3$ (C_{123})									
Shewhart	370.40	213.82	135.58	86.62	57.20	39.27	28.02	20.74	12.53	8.46	5.52	3.53	2.51	1.77	1.26	0.93	0.71
VSS	370.40	168.46	95.67	57.14	36.37	24.61	17.61	13.25	8.51	6.25	4.59	3.21	2.43	2.01	1.81	1.69	1.60
VSI	370.40	211.25	131.93	82.58	53.17	35.45	24.49	17.50	9.81	6.12	3.54	1.94	1.39	1.20	1.12	1.08	1.06
VSSI	370.40	**166.66**	**93.37**	**54.75**	**34.06**	**22.45**	**15.60**	**11.38**	6.88	4.57	2.80	1.76	1.40	1.24	1.16	1.13	1.10

Table 4. Comparison among the optimal $AATS(\delta)$ corresponding to the charts: $ATS(0) = 370.4$, $n_0 = 10$, $t_0 = 1$

	δ																
	0	0.1	0.15	0.2	0.25	0.3	0.35	0.4	0.5	0.6	0.75	1	1.25	1.5	1.75	2	2.25
								No rules (C_1)									
Shewhart	370.40	243.64	165.33	109.47	72.77	49.11	33.76	23.67	12.33	6.90	3.27	1.27	0.71	0.54	**0.51**	**0.50**	**0.50**
VSS	370.40	230.79	136.82	73.72	38.79	21.68	12.60	7.97	4.38	2.66	1.98	1.14	0.71	0.55	**0.51**	**0.50**	**0.50**
VSI	370.40	234.88	151.88	93.97	57.83	35.67	21.96	13.87	6.19	2.96	1.57	0.84	0.65	0.55	0.52	0.52	0.52
VSSI	370.40	223.77	127.78	64.74	31.80	15.78	8.67	5.45	**2.60**	**1.84**	1.60	**0.80**	0.70	0.54	**0.51**	**0.50**	**0.50**
								Rules $C1$, $C2$ (C_{12})									
Shewhart	370.40	190.33	111.87	66.69	41.34	26.80	18.18	12.48	6.58	4.02	2.30	1.24	0.81	0.59	**0.51**	**0.50**	**0.50**
VSS	370.40	156.87	83.61	46.48	27.50	17.37	11.69	7.94	4.30	2.87	1.97	1.38	0.82	0.75	0.58	0.51	**0.50**
VSI	370.40	187.31	110.02	64.33	39.49	25.38	20.48	13.65	6.67	3.72	1.85	0.85	**0.59**	**0.52**	**0.51**	0.51	0.51
VSSI	370.40	156.01	82.41	45.25	26.34	16.31	10.72	7.06	3.51	2.14	**1.40**	**0.80**	0.70	0.56	0.53	0.52	0.52
								Rules $C1$, $C2$, $C3$ (C_{123})									
Shewhart	370.40	146.71	78.05	44.48	27.40	18.14	12.82	9.58	6.14	4.50	3.24	2.00	1.23	0.81	0.59	0.52	**0.50**
VSS	370.40	111.36	54.80	30.32	18.73	12.74	9.42	7.47	5.44	4.42	3.48	2.59	2.19	1.97	1.80	1.69	1.60
VSI	370.40	143.19	73.99	40.58	23.89	15.04	10.07	7.12	4.07	2.69	1.75	1.24	1.12	1.07	1.05	1.04	1.04
VSSI	370.40	**102.89**	**48.53**	**25.75**	**15.24**	**9.92**	**7.03**	**5.36**	3.25	2.29	1.59	1.23	1.13	1.09	1.06	1.05	1.04

Table 5. Comparison among the optimal $AATS(\delta)$ corresponding to the charts: $ATS(0) = 499.6$, $n_0 = 3$, $t_0 = 1$

	δ																
	0	0.1	0.15	0.2	0.25	0.3	0.35	0.4	0.5	0.6	0.75	1	1.25	1.5	1.75	2	2.25
								No rules (C_1)									
Shewhart	499.60	430.71	365.75	299.50	240.15	190.61	150.80	119.43	75.76	49.10	26.78	10.96	5.13	2.71	1.60	1.05	0.77
VSS	499.60	418.86	334.83	236.48	150.80	90.22	53.21	32.43	14.14	9.14	5.86	3.46	2.77	1.72	1.27	1.06	0.95
VSI	499.60	426.73	356.66	285.93	223.80	171.95	130.81	99.86	56.93	32.96	15.83	4.86	2.37	1.43	0.89	**0.68**	0.90
VSSI	499.60	420.67	331.95	232.52	146.67	86.50	50.48	30.80	**13.84**	**8.78**	**4.67**	**2.24**	**1.46**	**0.94**	**0.82**	0.74	0.84
								Rules $C1$, $C2$ (C_{12})									
Shewhart	499.60	399.93	317.06	241.77	181.34	135.61	101.85	76.73	44.99	27.69	14.55	6.13	3.19	2.21	1.39	0.97	0.74
VSS	499.60	308.64	197.96	124.15	79.26	51.11	35.44	25.25	15.81	9.63	6.29	4.07	2.81	2.15	1.72	1.43	1.20
VSI	499.60	397.88	324.24	249.30	181.87	135.65	105.86	79.56	46.11	27.86	14.10	5.48	2.60	1.46	0.94	0.70	**0.59**
VSSI	499.60	300.88	197.82	123.98	79.10	52.32	36.17	27.04	14.54	9.68	6.21	3.49	2.30	1.72	1.41	0.88	0.77
								Rules $C1$, $C2$, $C3$ (C_{123})									
Shewhart	499.60	340.06	238.33	163.91	113.80	80.64	58.53	43.54	25.85	16.73	10.00	5.63	3.97	3.09	2.41	1.83	1.38
VSS	499.60	287.27	181.73	115.89	76.36	52.28	37.17	27.38	16.37	10.94	7.01	4.39	3.16	2.38	1.94	1.71	1.57
VSI	499.60	337.54	234.37	159.13	108.72	75.59	53.69	38.99	21.94	13.38	7.27	3.47	2.12	1.54	1.27	1.14	1.08
VSSI	499.60	**285.42**	**179.10**	**112.94**	**73.36**	**49.38**	**34.42**	**24.80**	14.10	8.89	5.24	3.02	2.23	1.82	1.56	1.39	1.27

Table 6. Comparison among the optimal $AATS(\delta)$ corresponding to the charts: $ATS(0) = 499.6$, $n_0 = 5$, $t_0 = 1$

	δ																
	0	0.1	0.15	0.2	0.25	0.3	0.35	0.4	0.5	0.6	0.75	1	1.25	1.5	1.75	2	2.25
								No rules (C_1)									
Shewhart	499.60	393.76	307.64	231.33	171.36	126.69	94.10	70.45	40.62	24.37	12.18	4.59	2.10	1.16	0.76	0.59	0.53
VSS	499.60	379.91	265.61	162.42	91.20	49.88	28.04	16.90	8.85	5.29	3.37	1.94	1.42	1.93	0.95	0.89	0.79
VSI	499.60	386.96	294.83	213.87	151.80	106.85	74.91	52.85	25.88	13.98	5.53	1.94	0.99	0.72	0.89	0.88	0.82
VSSI	499.60	376.44	259.41	155.40	84.80	44.74	24.32	14.74	7.30	4.76	**2.73**	**1.27**	**0.90**	**0.70**	0.69	0.61	0.57
								Rules $C1$, $C2$ (C_{12})									
Shewhart	499.60	352.14	250.78	172.88	118.75	82.38	58.05	41.65	22.70	13.33	6.82	3.59	1.65	1.06	0.74	0.59	0.53
VSS	499.60	273.13	158.58	96.32	58.85	37.59	25.21	17.35	9.41	6.05	3.84	2.36	1.68	1.29	1.00	0.79	0.65
VSI	499.60	349.09	246.81	168.76	114.90	78.93	55.02	39.01	20.71	11.80	5.74	2.26	1.17	0.77	**0.61**	**0.50**	**0.50**
VSSI	499.60	272.95	161.75	95.78	57.61	36.34	23.97	16.55	8.92	5.56	3.66	1.80	1.71	0.86	0.73	0.64	0.60
								Rules $C1$, $C2$, $C3$ (C_{123})									
Shewhart	499.60	277.88	171.86	107.38	69.49	46.83	32.85	23.94	14.09	9.32	5.96	3.80	2.77	1.97	1.37	0.98	0.74
VSS	499.60	209.80	114.33	66.06	40.92	27.08	19.04	14.13	8.94	6.50	4.59	3.09	2.22	1.76	1.57	1.57	1.38
VSI	499.60	274.44	167.15	102.29	64.52	42.20	28.63	20.13	10.95	6.67	3.75	1.99	1.39	1.17	1.08	1.03	1.01
VSSI	499.60	**207.46**	**111.50**	**63.22**	**38.25**	**24.63**	**16.79**	**12.06**	**7.14**	**4.67**	2.99	1.99	1.57	1.33	1.20	1.13	1.10

Table 7. Comparison among the optimal $AATS(\delta)$ corresponding to the charts: $ATS(0) = 499.6$, $n_0 = 10$, $t_0 = 1$

	δ																
	0	0.1	0.15	0.2	0.25	0.3	0.35	0.4	0.5	0.6	0.75	1	1.25	1.5	1.75	2	2.25
								No rules (C_1)									
Shewhart	499.60	322.10	215.24	140.48	92.16	61.42	41.72	28.91	14.73	8.08	3.73	1.39	0.74	**0.55**	**0.51**	**0.50**	**0.50**
VSS	499.60	303.49	175.23	91.74	46.92	24.74	13.96	8.68	4.79	2.79	1.80	1.17	0.91	0.72	0.59	0.53	0.51
VSI	499.60	309.96	197.73	120.84	72.71	43.88	26.79	16.85	6.96	3.44	1.88	**0.80**	0.88	0.85	0.81	0.80	0.80
VSSI	499.60	294.72	163.45	80.72	38.87	18.69	9.60	5.96	**2.76**	**1.87**	**1.21**	0.89	0.84	0.82	0.77	0.73	0.69
								Rules $C1$, $C2$ (C_{12})									
Shewhart	499.60	266.74	157.76	93.25	56.66	35.69	23.36	15.87	8.14	4.72	2.51	1.25	0.73	**0.55**	**0.51**	**0.50**	**0.50**
VSS	499.60	204.25	105.72	56.97	32.60	19.86	12.85	8.80	4.82	3.14	2.10	1.41	1.00	0.72	0.56	**0.50**	**0.50**
VSI	499.60	274.08	157.78	96.78	58.35	36.24	23.26	15.44	7.49	4.08	1.97	0.88	**0.61**	**0.55**	0.54	0.53	0.53
VSSI	499.60	205.60	105.04	56.42	32.14	19.47	12.51	8.50	4.57	2.92	1.89	1.23	0.89	0.67	0.55	**0.50**	**0.50**
								Rules $C1$, $C2$, $C3$ (C_{123})									
Shewhart	499.60	186.72	96.27	53.37	32.08	20.80	14.42	10.61	6.65	4.83	3.51	2.22	1.34	0.85	0.61	0.52	**0.50**
VSS	499.60	129.40	60.07	31.85	19.06	12.66	9.17	7.14	5.03	3.89	2.86	1.85	1.45	1.24	1.01	0.77	0.61
VSI	499.60	182.16	91.18	48.61	27.89	17.17	11.26	7.81	4.34	2.80	1.78	1.22	1.07	1.02	0.99	0.99	0.98
VSSI	499.60	**126.54**	**57.17**	**29.23**	**16.74**	**10.57**	**7.27**	**5.37**	3.21	2.23	1.61	1.24	1.11	1.06	1.03	1.01	0.99

then reflected to the adaptive schemes when the hybrid charts are considered. Furthermore, this synergistic effect allows the optimal interval to be extended to $\delta = 0.5$. Figures 3–8 graphically show this behaviour when $ATS(0)^* = 370.4$ or 499.6 and $n_0 = 3$, 5. Similar conclusions can be drawn for the other scenarios. Another interesting conclusion that can be deduced by the analysis

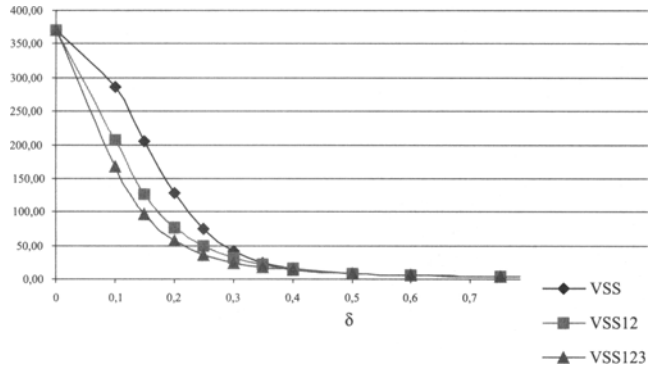

Fig. 3. $ATS(0) = 370.4$, $n_0 = 5$, $t_0 = 1$. Comparison among the $AATS(\delta)$ corresponding to the VSS schemes: simple (VSS), with rules $C1$ and $C2$ (VSS12) and with rules $C1$, $C2$ and $C3$ (VSS123)

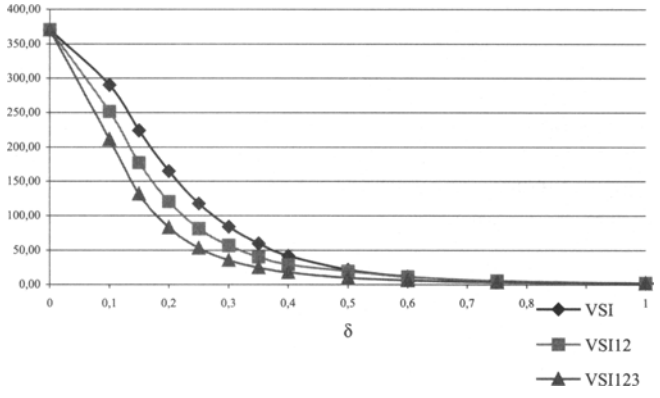

Fig. 4. $ATS(0) = 499.6$, $n_0 = 5$, $t_0 = 1$. Comparison among the $AATS(\delta)$ corresponding to the VSS schemes: simple (VSS), with rules $C1$ and $C2$ (VSS12) and with rules $C1$, $C2$ and $C3$ (VSS123)

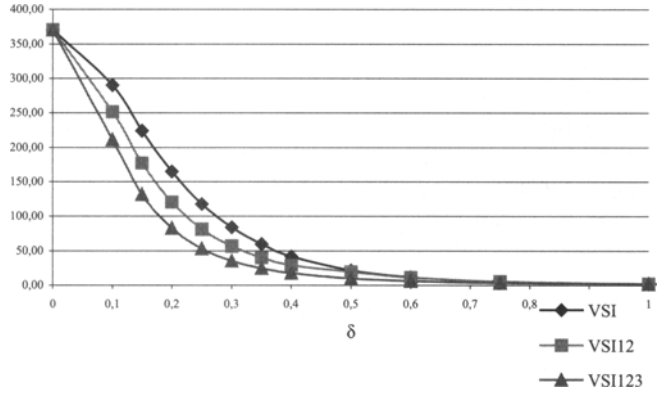

Fig. 5. $ATS(0) = 370.4$, $n_0 = 5$, $t_0 = 1$. Comparison among the $AATS(\delta)$ corresponding to the VSI schemes: simple (VSI), with rules $C1$ and $C2$ (VSI12) and with rules $C1$, $C2$ and $C3$ (VSI123)

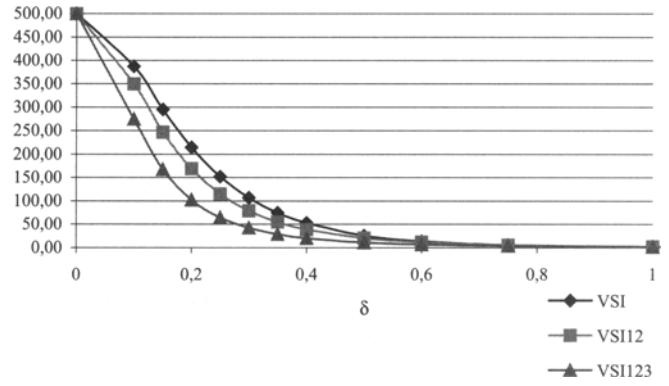

Fig. 6. $ATS(0) = 499.6$, $n_0 = 5$, $t_0 = 1$. Comparison among the $AATS(\delta)$ corresponding to the VSI schemes: simple (VSI), with rules $C1$ and $C2$ (VSI12) and with rules $C1$, $C2$ and $C3$ (VSI123)

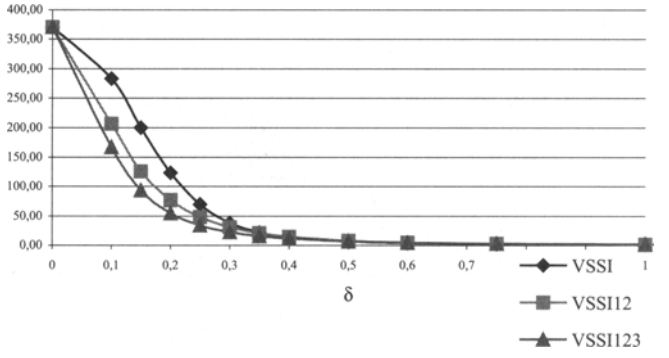

Fig. 7. $ATS(0) = 370.4$, $n_0 = 5$, $t_0 = 1$. Comparison among the $AATS(\delta)$ corresponding to the VSSI schemes: simple (VSSI), with rules $C1$ and $C2$ (VSSI12) and with rules $C1$, $C2$ and $C3$ (VSSI123)

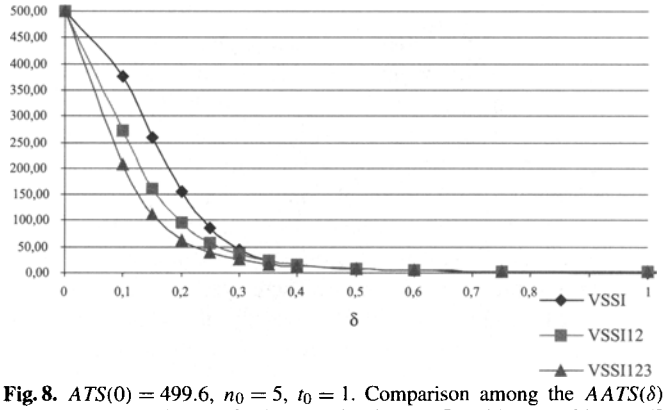

Fig. 8. $ATS(0) = 499.6$, $n_0 = 5$, $t_0 = 1$. Comparison among the $AATS(\delta)$ corresponding to the VSSI schemes: simple (VSSI), with rules $C1$ and $C2$ (VSSI12) and with rules $C1$, $C2$ and $C3$ (VSSI123)

of the results is that the possibility of varying sample size (VSS and VSSI) allows more performing charts to be implemented than with a variable sample interval (VSI) scheme. Furthermore, this tendency is not affected by the introduction of run rules. This aspect is shown in Figs. 9–10, which show $AATS(\delta)$ versus shift δ for adaptive charts with run rules assuming $ATS(0)^* = 370.4$, $n_0 = 5$ and $t_0 = 1$.

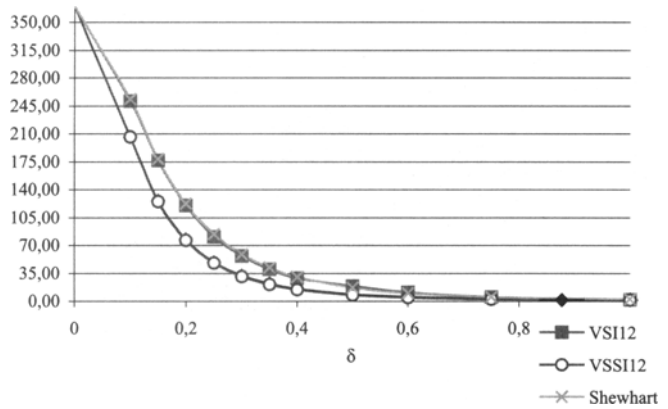

Fig. 9. $ATS(0) = 370.4$, $n_0 = 5$, $t_0 = 1$. Comparison among the $AATS(\delta)$ corresponding to the adaptive schemes with rules $C1$ and $C2$

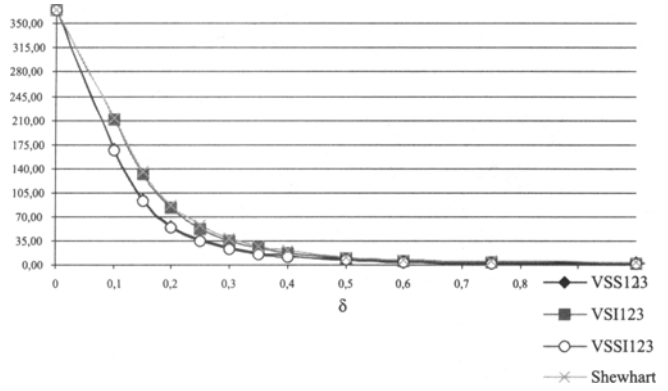

Fig. 10. $ATS(0) = 370.4$, $n_0 = 5$, $t_0 = 1$. Comparison among the $AATS(\delta)$ corresponding to the adaptive schemes with rules $C1$, $C2$ and $C3$

Once the positive effects of adding run rules to adaptive schemes with variable sample size and/or sampling interval have been demonstrated, a further interesting analysis examines the comparison with other kinds of control charts. In a recent publication, Carot et al. [24] proposed a chart, denoted as DSVSI, derived from the combination of a double sampling $\bar{X}$ chart (DS) with a variable sampling interval (VSI) approach. They show how such a new hybrid scheme outperforms the tradition adaptive and run rule Shewhart charts. Therefore, a comparison with the DSVSI scheme allows the efficiency of the proposed approach to be confirmed. In Tables 8 and 9, the results of this analysis are reported with respect to different scenarios. Furthermore, Table 9 shows a comparison with CUSUM and EWMA charts, in the same way as suggested by Carot et al. [24].

Table 8. Comparison of $AATS(\delta)$ for VSSI123 versus DSVSI ($ATS(0) = 370.4$, $n_0 = 4$, $t_0 = 1$)

Shift δ	DSVSI chart $(n_1, n_2) = (1, 16)$ $(h_1, h_2) = (0.25, 1.19)$ $(k_1, k_2) = (4.191, 2.596)$ $(w_n, w_l) = (1.318, 1.269)$	VSSI123 $(n_1, n_2) = (1, 11)$ $(h_1, h_2) = (0.1, 1.371)$ $(l, w, k) = (1.048, 2.678, 4.019)$
0	370.37	370.36
0.05	317.96	**303.20**
0.1	219.55	**192.88**
0.125	170.3	**149.4**
0.15	139.88	**115.71**
0.2	88.67	**71.00**
0.25	52.63	**45.48**
0.375	19.13	**18.12**
0.5	**8.45**	9.14
0.625	**4.49**	5.28
0.75	**2.79**	3.52
1	**1.51**	2.13
1.5	**0.92**	1.39
2	**0.94**	1.18

The obtained results show how the adaptive scheme with run rules allows a reduction of $AATS(\delta)$ for small shifts with respect to the DSVSI chart and the CUSUM (for moderate and large shifts, quite similar performances are provided) and allows equal results to be reached with respect to an EWMA scheme.

5 Conclusions

In this research, sample size and sampling interval adaptive $\bar{X}$ charts with run rules have been proposed to control the state of statistical control in a production process. The run rules were added to the adaptive schemes only for signalling purposes by considering sequences of non-consecutive plotted points. The performances of these charts were evaluated by determining their optimal statistical design and comparing it with that of other chart schemes commonly used in the literature. The optimal design was obtained by a heuristic algorithm; namely, simulated annealing, which works to determine the minimum $AATS(\delta)$ under the set of selected constraints. The obtained results show how the positive effects of adaptive chart parameters and run rules can be considered additive. The adaptive charts working together with run rules work better than the separated schemes when small to moderate shifts in the mean of the controlled parameter are expected. In particular, a combined sample size and sampling interval adaptive scheme added with western electric

Table 9. $ATS(0) = 250$, $n_0 = 3$, $t_0 = 3$. $AATS(\delta)$ for VSSI123, DSVSI, CUSUM and EWMA charts

	0	0.1	0.2	0.3	0.4	0.5	0.6	0.7	0.8	0.9	1
CUSUM	250	201.3	124.5	74.0	46.1	30.8	22.0	16.6	13.2	10.8	9.2
EWMA	250	188.8	108.1	62.6	**39.4**	**27.0**	**19.8**	**15.3**	**12.3**	**10.3**	**8.8**
DSVSI	250	195.0	115.4	67.0	41.5	27.9	20.3	15.7	12.9	10.9	9.6
VSSI123	250.4	**187.6**	**107.1**	**62.4**	39.5	27.1	19.8	15.4	12.5	10.6	9.3

rules $C1$, $C2$ and $C3$ has been demonstrated to be very effective, allowing large $AATS(\delta)$ reductions with respect to the other schemes when $\delta < 0.6$; when larger shifts are considered, the VSSI123 statistical performance remains quite similar to that of other charts. Furthermore, the statistical performance of this chart has also been compared with that of CUSUM and EWMA, i.e. charts that take into account the past history of the process. Once again, the results confirm the effectiveness of the proposed scheme.

References

1. Tagaras G (1998) A survey of recent developments in the design of adaptive control charts. J Qual Technol 12(3):212–231
2. Reynolds MR Jr, Amin RW, Arnold JC, Nachlas JA (1988) $\bar{X}$-charts with variable sampling intervals. Technometrics 30:181–192
3. Runger GC, Pigniatiello JJ Jr (1991) Adaptive sampling for process control. J Qual Technol 23(2):135–155
4. Runger GC, Montgomery DC (1993) Adaptive sampling enhancements for Shewhart control charts. IIE Trans 25(3):41–51
5. Reynolds MR Jr (1996) Shewhart and EWMA variable sampling interval control charts with sampling at fixed times. J Qual Technol 28(2):199–212
6. Das TK, Jain V, Gosavi A (1997) Economic design of dual-sampling interval policies for $\bar{X}$ charts with and without run rules. IIE Trans 29:497–506
7. Prabhu SS, Runger GC, Keats JB (1993) $\bar{X}$ chart with adaptive sample sizes. Int J Prod Res 31:2895–2909
8. Costa AFB (1994) $\bar{X}$ charts with variable sample size. J Qual Technol 26:155–163
9. Zimmer LS, Montgomery DC, Runger GC (1998) Evaluation of a three-state adaptive sample size $\bar{X}$ control chart. Int J Prod Res 36:733–743
10. Prabhu SS, Montgomery DC, Runger GC (1994) A combined adaptive sample size and sampling interval $\bar{X}$ control scheme. J Qual Technol 26(3):164–176
11. Costa AFB (1997) $\bar{X}$ chart with variable sample size and sampling intervals. J Qual Technol 29:197–204
12. Prabhu SS, Montgomery DC, Runger GC (1997) Economic-statistical design of an adaptive $\bar{X}$ chart. Int J Prod Econ 49:1–15
13. Western Electric (1956) Statistical quality control handbook. AT&T, Chicago
14. Parkhideh S, Parkhideh B (1996) The economic design of a flexible zone $\bar{X}$ chart with AT&T rules. IIE Trans 28(3):261–266
15. Parkhideh S, Parkhideh B (1998) Design of a flexible zone individuals control chart. Int J Prod Econ 36(8):2259–2267
16. Champ CW, Woodall WH (1990) A program to evaluate the run length distribution of a Shewhart control chart with supplementary run rules. J Qual Technol 22(1):68–73
17. Amin RW, Letsinger WC (1991) Improved switching rules in control procedures using variable sampling intervals. Commun Stat Simul Comput 20:205–230
18. Amin RW, Hemashina R (1993) The switching behaviour of $\bar{X}$ charts with variable sampling intervals. Commun Stat Theory Methods 22:2081–2102
19. Cui RQ, Reynolds MR Jr (1988) $\bar{X}$ -charts with run rules and variable sampling intervals. Commun Stat Simul Comput 17:1073–1093
20. Artiles-Leòn N, David HT, Meeks HD (1996) Statistical optimal design of control charts with supplementary stopping rules. IIE Trans 28(3):225–236
21. Kirkpatrick S, Gelatt CD, Vecchi MP (1983) Optimisation by simulated annealing science 220:671–680
22. Campisi S, Celano G, Costa A, Fichera S (2001) Economic design of a X adaptive control chart with run rules. In: Proceedings of the 16th International Conference on Production Research
23. Zimmer LS, Montgomery DC, Runger GC (2000) Guidelines for the application of adaptive control charting schemes. Int J Prod Res 38(9):1977–1992
24. Carot V, Jabaloyes M, Carot T (2002) Combined double sampling and variable sampling interval $\bar{X}$ chart. Int J Prod Res 40(9):2175–2186